Hyperfine and optical barium ion qubits

M. R. Dietrich,* N. Kurz, T. Noel, G. Shu, and B. B. Blinov
University of Washington Department of Physics, Seattle, Washington 98195, USA
(Received 1 April 2010; published 20 May 2010)

State preparation, qubit rotation, and high fidelity readout are demonstrated for two different $^{137}Ba^{+}$ qubit types. First, an optical qubit on the narrow $6S_{1/2}$ to $5D_{5/2}$ transition at 1.76 μm is implemented. Then, leveraging the techniques developed there for readout, a ground-state hyperfine qubit using the magnetically insensitive transition at 8 GHz is accomplished.

DOI: 10.1103/PhysRevA.81.052328 PACS number(s): 03.67.Lx, 32.80.Qk, 32.80.Fb, 37.10.Ty

I. INTRODUCTION

A quantum computer, once implemented, is expected to have several applications with significant scientific and social utility due to its ability to execute specific algorithms with scaling laws quadratically or exponentially faster than any known classical algorithm that accomplishes the same task [1]. The fundamental unit of information in a quantum computer is the qubit, which is physically realized by any coherent quantum two-level system. At present, the best-developed qubit technology is provided by the hyperfine or optical levels of an elemental ion suspended in a radio frequency (rf) Paul trap [2]. That fact is in no small part thanks to decades of development of techniques in atomic physics to manipulate these profoundly quantum systems.

Despite a long history in ion trapping [3–5], barium has never previously been demonstrated as an ionic qubit. Ba^{+} has several desirable characteristics for an ionic qubit. The odd isotope $^{137}Ba^{+}$ is relatively abundant at 11%, which is sufficiently high that it can be trapped from a natural source without isotope-selective ionization [6,7]. Barium possesses a long-lived metastable state $5^2D_{5/2}$ (see Fig. 1), whose lifetime (35 s) is an order of magnitude greater than that of any other singly ionized alkali-earth-metal atom [8]. It is important for this state to be long lived since that decay rate restricts the qubit readout fidelity and sets a physical upper limit to optical qubit coherence times. Furthermore, the laser wavelengths for the $6S_{1/2}$ to $5D_{5/2}$ infrared "shelving" transition as well as barium's visible-wavelength cooling transition are the longest of any ionic qubit candidate, which makes it favorable for remote photonic coupling through optical fiber. This property is essential for long distance entanglement between ionic qubits [9,10], since the postselection entanglement process is mediated by emitted photons. Current experiments are partly limited by attenuation of these photons in the optical fiber, an effect which is greatly reduced at longer wavelengths [11].

Here we report the trapping, state preparation, state rotation, and readout of two different $^{137}Ba^{+}$ ionic qubits, one based on the narrow infrared optical transition at 1.76 μm and the other based on the ground-state hyperfine splitting. In the former case, sufficient coherence is observed in the quadrupole transition in a Doppler-cooled ion to drive about 10 Rabi rotations. Since the excited $D_{5/2}$ state is disjoint from the laser cooling cycle, readout is effected by simply enabling the cooling lasers and looking for fluorescence. In the latter case, qubit rotations are driven by a resonant microwave radiation pulse near 8 GHz and readout is achieved directly with Rabi oscillation on the 1.76-μm transition to selectively shelve the ion into the metastable state.

II. EXPERIMENTAL SETUP

The energy level diagram for $^{137}Ba^{+}$ can be found in Fig. 1. The ion is Doppler cooled on the $D1$ line at 493 nm using a frequency-doubled 986-nm external cavity diode laser (ECDL). Since this state decays into the $D_{3/2}$ state about 25% of the time, the ion must then be repumped out using a second ECDL at 650 nm. $^{137}Ba^{+}$ has a nuclear spin of $I = 3/2$; in order to optically address all hyperfine levels in the S and D states, the 493-nm laser beam is modulated with an electro-optic modulator (EOM) at 8.037 GHz, while the 650-nm laser is directly current modulated at 614, 539, and 394 MHz using a bias-T. The 493-nm laser carrier is set to the $F = 1 \rightarrow F' = 2$ transition while the sideband drives $F = 2 \rightarrow F' = 2$, where the prime indicates the $P_{1/2}$ manifold. This configuration avoids the weak $F = 1 \rightarrow F' = 1$ transition and allows us to optically pump into the state $F = 2, m_F = 0$ using π-polarized light. For optimal cooling, the 493-nm laser is set to an elliptical polarization.

The 986-nm laser is frequency stabilized using an Invar-spaced optical cavity with a free spectral range of 1.2 GHz and finesse of about 150, which is in a sealed, temperature controlled cylinder. A frequency shift is provided by a double-passed acousto-optic modulator (AOM), whose feed rf is frequency modulated. We then detect the transmitted laser power and use a lock-in amplifier to extract an error signal, which is fed back to the laser. The 650-nm laser is monitored by a commercial wavelength meter (Highfinesse WS7) and stabilized via feedback from the computer attached to the wavelength meter [12].

The trap is loaded using isotope-selective two-step photoionization with a 791-nm ECDL and a N_2 laser [7]. This allows us to easily switch between $^{137}Ba^{+}$ and the more common $^{138}Ba^{+}$ isotope for use in various experiments. Improved reliability and trapping lifetimes have been observed using this technique when compared to trapping $^{137}Ba^{+}$ without selective photoionization. It is not uncommon to hold an ion now for several days, where previously the lifetime in our trap for $^{137}Ba^{+}$ was measured in hours. Our Paul trap is a linear design with 670 volts applied to needle endcaps separated by 3.2 mm, similar to the one described in Ref. [13],

*dietricm@u.washington.edu

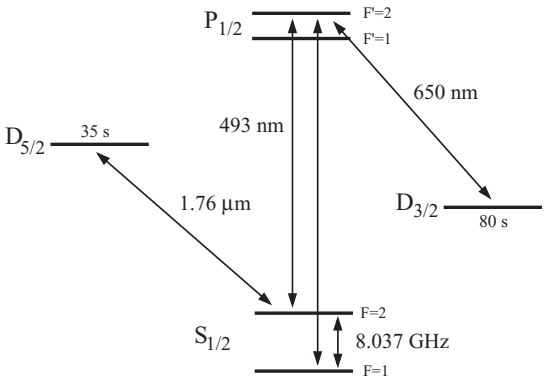

FIG. 1. A representation of the energy levels in $^{137}Ba^{+}$, and the transitions accessed by various lasers. The ion is cooled on the 493-nm transition with 8.037-GHz sidebands and repumped with a 650-nm laser diode. Shelving to the $D_{5/2}$ state is accomplished through coherent excitation with the 1.76-μm laser. Hyperfine structure of the D states is not shown.

driven with 5 watts of rf at 12.39 MHz. The trap has an axial secular frequency of about 600 kHz and radial frequencies 1.43 and 2.58 MHz. A dc magnetic field of 8.9 G created by two current-carrying coils is made parallel with the cooling laser and perpendicular to the optical pumping beam. This field is necessary to break degeneracies and prevent the cooling laser from pumping the ion into a dark state formed by a superposition of Zeeman levels.

The ion can be optically pumped into the $F = 2, m_F = 0$ state by relying on the forbidden $F = 2, m_F = 0 \rightarrow F' = 2, m_F = 0$ transition. Thus, by setting the optical pumping beam to have a linear polarization aligned with the magnetic field, corresponding to π polarization, the ion is observed to optically pump into the $F = 2, m_F = 0$ state after less than 100 μs of exposure time with $93\% \pm 1\%$ fidelity. Further optimization of the pump-laser polarization is needed to achieve better pumping.

While the ion is excited into the $D_{5/2}$ state, it is removed from the cooling cycle and will appear dark when the ion is exposed to the cooling lasers which normally cause fluorescence [14]. This bright-dark signal is the basis of our qubit readout. Due to the long shelved state lifetime, it is expected that we can obtain extremely high detection fidelities, using for example adaptive techniques [15] and high numerical-aperture optics [16–18]. We excite the ion directly into the dark state using a 1.76-μm fiber laser frequency referenced to a temperature-controlled Zerodur^{TM} cavity located in a chamber evacuated to 10^{-7} Torr. The cavity has a free spectral range of 500 MHz and a finesse of 1000. By direct measurement of the 1.76-μm transition width in Ba^{+}, the laser linewidth is found to be no larger than 10 kHz. With a typical ion brightness of about 2100 photon counts per second, we obtain better than 99% bright-dark-detection fidelity in 10 ms (see Fig. 2). This rate of fluorescence detection is to be expected from the spontaneous decay rate of about 20 MHz along with our numerical aperture of 0.22 and photo-multiplier-tube quantum efficiency of 11%.

The optical setup for the 1.76-μm laser can be found in Fig. 3. Half of the total beam power is diverted to the laser-stabilization setup, while the other half is used to drive

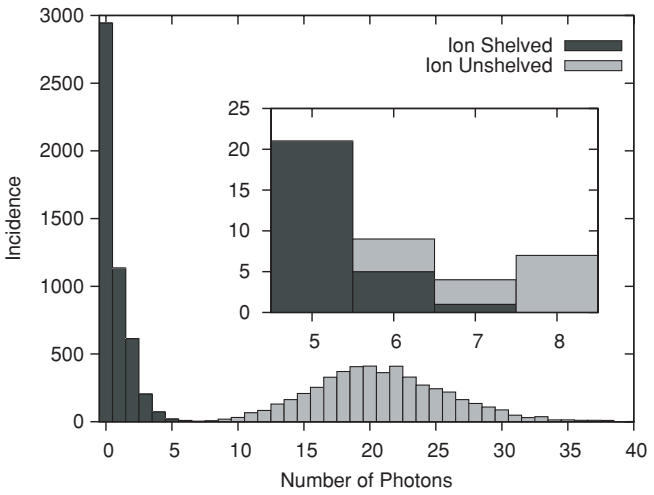

FIG. 2. A histogram of ion brightness for two cases; where the ion has been deliberately shelved by disabling the red laser (dark) and where it has not (light). Each case has 5000 data points, and represents a cooling-laser exposure time of 10 ms. The inset shows a zoom in of the overlap region at 6 and 7 photon counts. In this region, there are 13 offending events out of a total of 10 000 runs, corresponding to a detection fidelity of 99.87%.

the ion. The beam used for laser stabilization is double-passed through an AOM which is used both to shift the laser frequency with respect to the cavity resonance and to introduce frequency modulation needed for the Pound-Drever-Hall (PDH) lock [19,20]. The beam intended to drive the ion is focused into an identical AOM, and then two lenses effectively image this focus onto the ion location. This configuration allows us to adjust the AOM frequency without the beam shifting off the ion's location.

To generate the PDH error signal, rf is created by a synthesizer and mixed with a 1-MHz sine wave and a dc voltage in an I-Q modulator. This allows high-bandwidth frequency modulation on the output of a synthesized rf signal [12]. This modulation is then mapped onto the 1.76-μm laser by application of the double-passed AOM. With frequency modulation, it is then possible to observe a PDH error signal

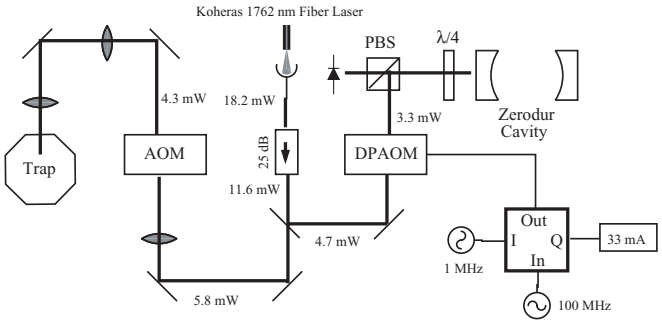

FIG. 3. The optical setup for the 1.76-μm laser. The laser power is split between laser stabilization and ion state manipulation. The laser is servo locked to a Zerodur-spaced cavity using a Pound-Drever-Hall technique, where frequency modulation is introduced by a double-passed AOM (DPAOM), whose drive frequency is modulated by an in-phase–quadrature (I-Q) modulator. The laser light intended for the ion is switched and frequency shifted by a separate AOM.

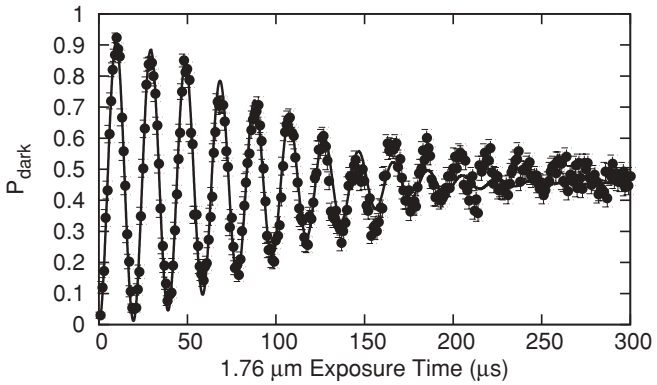

FIG. 4. Coherent excitation of the 1.76-μm transition. The probability of detecting the ion in the dark state is plotted against the time for which the laser is exposed to the ion. Readout is accomplished in about 20 ms by activating the cooling lasers. The Rabi frequency is observed to be about 50 kHz with a decay time of 120 μs. These parameters were determined by a least-squares fit to a sine wave with a Gaussian decay envelope, which is shown by the solid line.

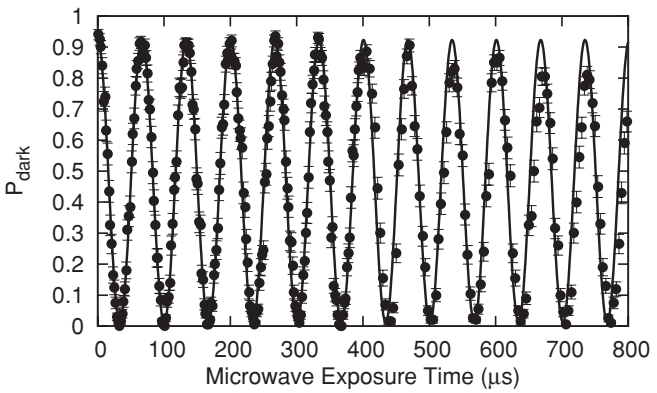

FIG. 5. The qubit state after an 8-GHz resonant pulse. The maximum probability of a dark ion is limited by optical pumping and the shelving efficiency, while the minimum is limited by coherence of the hyperfine qubit. At longer exposure times, the maximum shelving probability is seen to decrease due to magnetic noise of the 1.76-μm transition, while the minimum probability remains 0%. The Rabi frequency is 15 kHz, again obtained through a fit, which is shown as a solid line.

from the retroreflected beam of the Zerodur cavity without resorting to an EOM.

III. RESULTS

In a field stronger than about 1 G, the 500-kHz splitting of the $D_{5/2}, F = 3, F = 4$ hyperfine levels [21] is overcome so that they become an effective $J = 4$ manifold [22]. In our experiments, it is into the $J = 4, m_J = -2$ level (formed from an $m_F = -1$ and an $m_F = -3$ level) that the 1.76-μm laser drives the ion from the ground state $F = 2, m_F = 0$. These two states constitute the levels of our optical qubit. Coherent optical nutation on this transition can be seen in Fig. 4. The measured Rabi frequency is about 50 kHz using 4.3 mW of laser power focused to an intensity of roughly 60 W/cm^2, and a decay time of about 120 μs is observed. In order to obtain this curve, the ion was first optically pumped, then exposed to 1.76-μm light for a fixed period of time, and finally the cooling lasers were enabled and fluorescence was detected. In order to suppress dephasing due to magnetic field fluctuations, the infrared laser exposure was triggered on the rising slope of the 60-Hz ac power line voltage. Although the coherence time is roughly consistent with the laser linewidth, expected to be about 10 kHz, changes in the coherence time have been observed by adjusting the ion temperature through manipulation of the cooling laser frequency. This suggests that increased coherence might be observed with improved ion cooling.

Once a robust readout mechanism is developed, it is possible to use the hyperfine structure of $^{137}Ba^+$ as a qubit [23]. By exposing the ion to a π pulse of 1.76-μm light, we can selectively excite the ion from the $|0\rangle$ qubit state into the shelved state. An alternative method would be to use adiabatic passage, which offers more robust population transfer [24]. This technique has also been developed, but is not implemented here. Using the magnetically insensitive $m_F = 0$ levels of the two ground-state hyperfine levels as our qubit states, coherence times of many seconds can be achieved [13,25,26]. Qubit rotations were obtained by directly exposing the ion to 10 W of resonant microwave radiation at approximately 8 GHz [27,28] after being optically pumped. Then, the 1.76-μm laser is applied to shelve the ion if it is in the higher energy state $F = 2, m_F = 0$, but not in any other hyperfine level, then finally the cooling lasers are activated and fluorescence is detected. As can be seen in Fig. 5, this procedure results in Rabi flops with a frequency of 15 kHz. Although the entire sequence was line triggered, the increasing length of the microwave pulse caused the 1.76-μm laser pulse to occur at a later time in the sequence. This resulted in the laser frequency slipping off resonance somewhat, since the pulse began at a different ac phase. This accounts for the diminishing readout efficiency at longer microwave exposure times. Decoherence in the hyperfine qubit itself would appear as an increasing minimum probability, which is not resolved within 800 μs.

IV. CONCLUSION

Herein we have demonstrated two implementations of ionic qubits using $^{137}Ba^+$, first an optical qubit, and then a hyperfine qubit that takes advantage of the techniques developed for the optical qubit for readout. Because of the long wavelengths involved, it is expected that this advance will facilitate future developments in ion-photon and long-distance ion-ion entanglement, which in turn is vital for quantum information processing, loop-hole-free Bell inequality tests [9], and quantum repeaters for cryptographic applications [29]. In the immediate future, we intend to pursue these goals through improved fluorescence capture and simplified ion-photon entanglement techniques. First, improved collection of ion fluorescence and fiber coupling will greatly increase the rate of entanglement over previous experiments. Also, we will use our optical rotations to demonstrate a Zeeman qubit in $^{138}Ba^+$, since the simplicity of that atomic system promises to make ion-photon entanglement much easier.

ACKNOWLEDGMENTS

We would like to acknowledge the technical assistance of a number of people, including Joanna Salacka, Aaron Avril, Ryan Bowler, Adam Kleczewski, Joseph Pirtle, Chris Dostert, Frank Garcia, Sanghoon Chong, Tom Chartrand, Viki Mirgon, Eric Magnuson, Peter Greene, Jennifer Porter, Anya Davis, Corey Adams, and Edan Shahar. This research was supported by the National Science Foundation Grants No. 0758025 and No. 0904004, and the Army Research Office under the DURIP program.

[1] M. A. Nielsen and I. L. Chuang, *Quantum Computation and Quantum Information* (Cambridge University Press, Cambridge, 2000).

[2] T. D. Ladd, F. Jelezko, R. Laflamme, Y. Nakamura, C. Monroe, and J. L. O'Brien, Nature (London) **464**, 45 (2010).

[3] W. Neuhauser, M. Hohenstatt, P. E. Toschek, and H. Dehmelt, Phys. Rev. A **22**, 1137 (1980).

[4] G. Janik, W. Nagourney, and H. Dehmelt, J. Opt. Soc. Am. B **2**, 1251 (1985).

[5] R. G. DeVoe and C. Kurtsiefer, Phys. Rev. A **65**, 063407 (2002).

[6] M. R. Dietrich, A. Avril, R. Bowler, N. Kurz, J. S. Salacka, G. Shu, and B. B. Blinov, in *Non-Neutral Plamsa Physics VII*, edited by J. R. Danielson and T. S. Pedersen (AIP Conference Proceedings No. 1114, 2008), p. 25.

[7] A. V. Steele, L. R. Churchill, P. F. Griffin, and M. S. Chapman, Phys. Rev. A **75**, 053404 (2007).

[8] A. A. Madej and J. D. Sankey, Phys. Rev. A **41**, 2621 (1990).

[9] C. Simon and W. T. M. Irvine, Phys. Rev. Lett. **91**, 110405 (2003).

[10] S. Olmschenk, D. N. Matsukevich, P. Maunz, D. Hayes, L.-M. Duan, and C. Monroe, Science **323**, 486 (2009).

[11] D. L. Moehring, M. J. Madsen, B. B. Blinov, and C. Monroe, Phys. Rev. Lett. **93**, 090410 (2004).

[12] M. Dietrich, Ph.D. thesis, University of Washington, 2009. Downloadable at [http://depts.washington.edu/qcomp/theses.html]. Information regarding the wavelength-meter-based lock can be found in section 7.2, and the I-Q modulation scheme in section 11.2.

[13] S. Olmschenk, K. C. Younge, D. L. Moehring, D. Matsukevich, P. Maunz, and C. Monroe, Phys. Rev. A **76**, 052314 (2007).

[14] W. Nagourney, J. Sandberg, and H. Dehmelt, Phys. Rev. Lett. **56**, 2797 (1986).

[15] A. H. Myerson, D. J. Szwer, S. C. Webster, D. T. C. Allcock, M. J. Curtis, G. Imreh, J. A. Sherman, D. N. Stacey, A. M. Steane, and D. M. Lucas, Phys. Rev. Lett. **100**, 200502 (2008).

[16] S. Gerber, D. Rotter, M. Hennrich, R. Blatt, F. Rohde, C. Schuck, M. Almendros, R. Gehr, F. Dubin, and J. Eschner, New J. Phys. **11**, 013032 (2009).

[17] C. Raab, J. Eschner, J. Bolle, H. Oberst, F. Schmidt-Kaler, and R. Blatt, Phys. Rev. Lett. **85**, 538 (2000).

[18] G. Shu, M. R. Dietrich, N. Kurz, and B. B. Blinov, J. Phys. B **42**, 154005 (2009).

[19] E. D. Black, Am. J. Phys. **69**, 79 (2001).

[20] R. W. P. Drever, J. L. Hall, F. V. Kowalski, J. Hough, G. M. Ford, A. J. Munley, and H. Ward, Appl. Phys. B **31**, 97 (1983).

[21] R. E. Silverans, G. Borghs, P. De Bisschop, and M. Van Hove, Phys. Rev. A **33**, 2117 (1986).

[22] K. Beloy, A. Derevianko, V. A. Dzuba, G. T. Howell, B. B. Blinov, and E. N. Fortson, Phys. Rev. A **77**, 052503 (2008).

[23] G. Kirchmair, J. Benhelm, F. Zähringer, R. Gerritsma, C. F. Roos, and R. Blatt, Phys. Rev. A **79**, 020304(R) (2009).

[24] C. Wunderlich, T. Hannemann, T. Körber, H. Häffner, C. Roos, W. Hänsel, R. Blatt, and F. Schmidt-Kaler, J. Mod. Opt. **54**, 1541 (2007).

[25] H. Häffner *et al.*, Appl. Phys. B **81**, 151 (2005).

[26] D. J. Berkeland, J. D. Miller, J. C. Bergquist, W. M. Itano, and D. J. Wineland, J. Appl. Phys. **83**, 5025 (1998).

[27] R. Blatt and G. Werth, Phys. Rev. A **25**, 1476 (1982).

[28] W. Becker, R. Blatt, and G. G. Werth, J. Phys. Colloques **42**, C8-339 (1981).

[29] L.-M. Duan, M. D. Lukin, J. I. Cirac, and P. Zoller, Nature (London) **414**, 413 (2001).